of nuclear model is arbitrary. The radii are given here for a uniform nuclear charge distribution, constant within $R$ and zero outside $R$, where

$$R=r_0A^{\frac{1}{3}}\times10^{-13}\text{ cm}.$$

The results are $r_0=1.14\pm0.15$ at 31 Mev, $r_0=1.19\pm0.09$ at 40 Mev, and $r_0=1.21\pm0.18$ at 60 Mev. The value of $r_0$ for the combined data is $1.18\pm0.10$.

The radius of the tungsten nucleus given here is significantly larger than the value reported in the earlier paper,[1] $R=(1.0\pm0.1)A^{\frac{1}{3}}\times10^{-13}$ cm. The data in the previous experiments were corrected for very high background levels, and it appears certain that this correction introduced a systematic error comparable with the statistical error in the experiment. The background in the present experiment was never greater than 0.2% of the signal counting rate.

## CONCLUSION

A recent analysis has shown that the root-mean-square radius of the nuclear charge distribution determines the electron scattering cross section for energies as high as 60 Mev. No significantly different information is expected, therefore, at the three energies, 31, 40, and 60 Mev, which were selected in this experiment. In fact, either an absolute cross section measurement at one angle and one energy or a ratio of counting rates for two angles and one energy would be sufficient to determine root-mean-square radius. The results at other angles and energies serve only as checks for internal consistency in the theory. A root-mean-square radius equal to $(0.91\pm0.10)A^{\frac{1}{3}}\times10^{-13}$ predicts the observed angular distributions at all three energies. There are several sources of error in the present phase-shift calculations of the electron scattering cross section. The scattering nucleus is represented by a static, continuous electric charge distribution. Both virtual and real excitation of the nucleus in the scattering event are ignored. Finally, no radiative correction is applied at high energies. It is concluded from this experiment that these factors would not alter the angular distributions predicted by the simple scattering model by more than 10%.

## ACKNOWLEDGMENTS

The authors would like to thank H. Feshbach and A. E. Glassgold for the use of their scattering calculations prior to publication and for the special computation of phase shifts for $Z=74$.

PHYSICAL REVIEW VOLUME 99, NUMBER 5 SEPTEMBER 1, 1955

# Elastic Scattering of Alpha Particles and Deuterons by Complex Nuclei*

C. E. PORTER
*Brookhaven National Laboratory, Upton, Long Island, New York*
(Received May 25, 1955)

The elastic scattering of alpha particles and deuterons by heavy nuclei is calculated approximately using a classical approach. Rough agreement with the available alpha particle data is obtained with a ratio of interaction radius to mean free path near the center of the nucleus of about 3 to 4 and a $(1/e)$ edge-diffuseness distance of $1\times10^{-13}$ cm. Interpretation of the available deuteron data is somewhat uncertain at present.

## I. INTRODUCTION

WITHIN the past few years there has been a revival of interest in the elastic scattering of alpha particles and deuterons from heavy nuclei. Experiments[1–4] for alpha particles have been carried out at energies ranging from 20 to 40 Mev with essentially complete angular coverage at a few energies. For deuterons, angular distributions have been measured at 15 Mev.[5] The main feature that the various sets of data have in common is the approximately exponential drop of the scattered intensity from the Coulomb value, beginning at a specific energy in the measurements made at a fixed angle as a function of beam energy and beginning at a specific angle in angular distributions measured at a given beam energy. A number of discussions of the interpretation of the alpha-particle data have been given.[3,6–8]

It has been emphasized by Wegner[9] that the alpha-particle data can be most easily understood by plotting both the energy dependent and angular dependent data as a function of the apsidal distance $D$ (distance of closest approach) of the hyperbolic Coulomb orbit. On

* Work carried out under contract with U. S. Atomic Energy Commission.

[1] H. E. Gove, Massachusetts Institute of Technology, Laboratory for Nuclear Science and Engineering Progress Report, May 31, 1951 (unpublished), p. 157.
[2] G. W. Farwell and H. E. Wegner, Phys. Rev. **95**, 1212 (1954).
[3] Wall, Rees, and Ford, Phys. Rev. **97**, 726 (1955).
[4] Wegner, Eisberg, and Igo, Phys. Rev. **99**, 825 (1955).
[5] H. E. Gove, Massachusetts Institute of Technology, Laboratory for Nuclear Science and Engineering Progress Reports, July 1, 1950 (unpublished), p. 139; February 28, 1951 (unpublished), p. 40; and private communication.
[6] J. S. Blair, Phys. Rev. **95**, 1218 (1954).
[7] K. Izumo, Progr. Theoret. Phys. (Japan) **12**, 549 (1954).
[8] K. W. Ford and J. A. Wheeler (private communication via H. E. Wegner).
[9] H. E. Wegner, Brookhaven National Laboratory Report BNL-331, 1955 (unpublished), p. 56; and private communication.

such a plot, both types of data coincide over a drop below the Coulomb scattering of a few orders of magnitude. This can be seen in the experimental points plotted in Figs. 3–7. None of the theoretical discussions[3,6–8] given so far has focused on this simple feature of the data, and except for the recent work of Ford and Wheeler,[8] the predicted drop below Coulomb disagrees badly with the 40-Mev data[4] at backward angles. The calculations of Ford and Wheeler, although exhibiting the rapid drop of the data, do not join properly to the Coulomb scattering at the break angle. If these calculations are normalized to the Coulomb scattering at the break angle, then the predicted drop from Coulomb is much too rapid when compared to the measured results.

## II. THEORY

Since $(R/\lambda\!\!\!^{-})$, where $R$ is the interaction radius and $\lambda\!\!\!^{-}$ is the alpha particle or deuteron wavelength divided by $2\pi$, is very large ($\sim$20 for alphas and $\sim$10 for deuterons) for the data mentioned above, the scattering can be calculated approximately using a classical point of view. To simplify the calculation, we assume that the main effect that lowers the cross section is absorption of the alpha particle or deuteron from the incident beam. In addition to this, it is assumed that the Coulomb orbits are not distorted by the nucleus. The abrogation of these assumptions is considered to be a refinement. We now argue that the decrease in scattered intensity as a function of apsidal distance comes entirely from absorption along the Coulomb orbit, and hence we write for the actual cross section in terms of the Coulomb cross section

$$d\sigma_{el}/d\Omega=(d\sigma_{el}/d\Omega)_{coul}T, \tag{1}$$

where $T$ is a transmission factor giving the fraction of the incident beam that emerges from the nucleus.[10] $T$ has the form

$$T=\exp\left(-\int\frac{dx}{l(x)}\right), \tag{2}$$

with $x$ the coordinate along the path of the alpha particle or deuteron and $l(x)$ the mean free path as a function of position along the path.

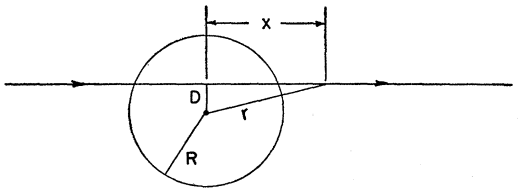


FIG. 1. Path geometry for a straight line path. $R$ is the interaction radius, $r$ and $x$ are path coordinates, and $D$ is the apsidal distance.

[10] The approach here does not differ essentially from that of Fernbach, Serber, and Taylor, Phys. Rev. 75, 1352 (1949).

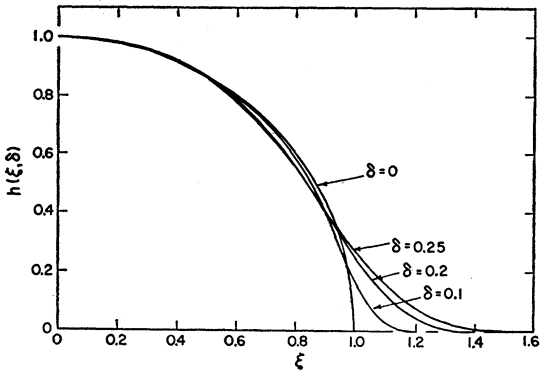


FIG. 2. Plot of $h(\xi,\delta)$ as a function of $\xi=D/R$ for various values of $\delta=d/R$, *viz.*, $\delta=0$, 0.1, 0.2, and 0.25.

We now calculate $T$ for an oversimplified model in which the paths through the nucleus are assumed to be straight lines. Equation (2) can be written

$$\int\frac{dx}{l(x)}=2\int_{r=D}^{r=\infty}dr\left(\frac{dx}{dr}\right)\frac{1}{l(r)}, \tag{3}$$

where $r$ is the radial coordinate of the orbit as shown in Fig. 1. On integrating by parts, Eq. (3) becomes

$$\int\frac{dx}{l(x)}=2\int_{D}^{\infty}drx(r)\frac{d}{dr}\left(\frac{-1}{l(r)}\right), \tag{4}$$

since

$$\begin{aligned} x&=0 \quad \text{for} \quad r=D,\\ (1/l)&\to 0 \quad \text{for} \quad r\to\infty. \end{aligned} \tag{5}$$

Now $l(r)$ is proportional to the reciprocal of the particle density in the nucleus. If we assume a form for this density that has been used widely, *viz.*,

$$\rho(r)=\rho_0\times\frac{1}{2}\left(1-\tanh\frac{r-R}{d}\right), \tag{6}$$

where $d$ is a measure of the thickness of the diffuse edge and $R$ is the interaction radius, then

$$\frac{1}{l}=\frac{1}{l_0}\times\frac{1}{2}\left(1-\tanh\frac{r-R}{d}\right). \tag{7}$$

In this equation, $l_0$ is the mean free path near the center of the nucleus. For a sharp-edged interaction region

$$\frac{d}{dr}\left(\frac{-1}{l(r)}\right)\underset{d\to 0}{\to}\frac{1}{l_0}\delta(r-R), \tag{8}$$

which supplies the motivation for the partial integration performed on Eq. (3). With the assumption of straight line paths (see Fig. 1)

$$x(r)=(r^2-D^2)^{\frac{1}{2}}, \tag{9}$$

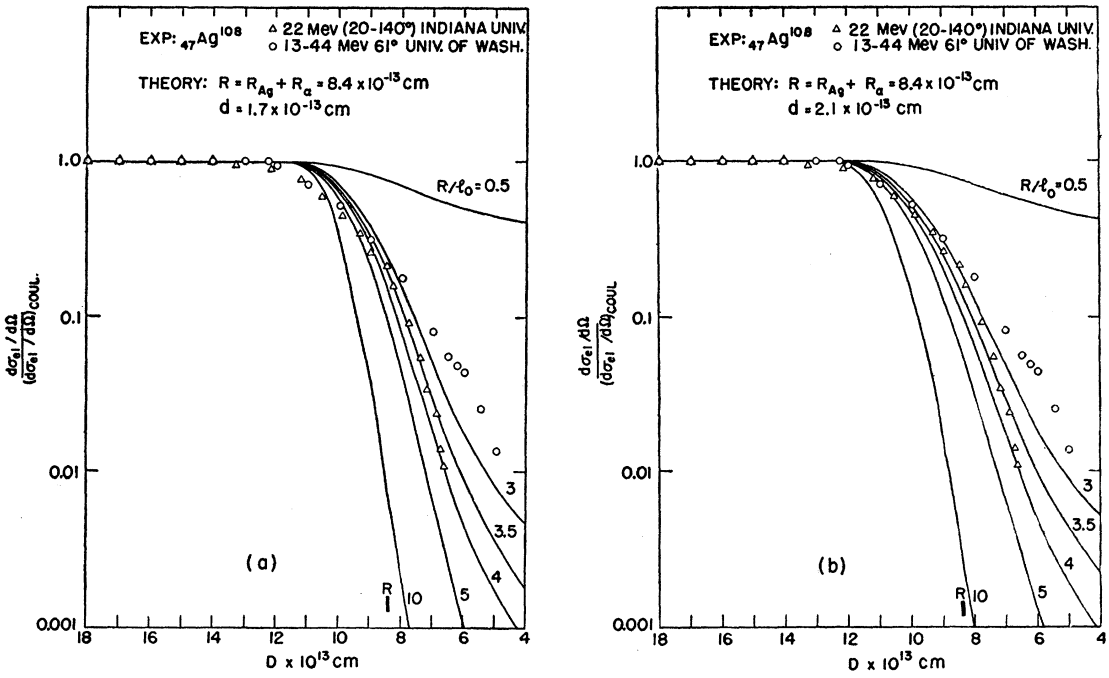


FIG. 3. Plot of differential elastic scattering cross section divided by the differential Coulomb cross section *versus* apsidal distance for $_{47}Ag^{108}$. The triangles are data for 22-Mev alpha particles with scattering angles ranging from 20° to 140° (reference 3). The open circles are data for 13- to 44-Mev alpha particles at a scattering angle of 61° (reference 2). Theoretical curves are shown for $R=8.4\times10^{-13}$ cm, $R/l_0=0.5$, 3, 3.5, 4, 5, and 10, and (a) $d=1.7\times10^{-13}$ cm ($\delta=0.2$); (b) $d=2.1\times10^{-13}$ cm ($\delta=0.25$).

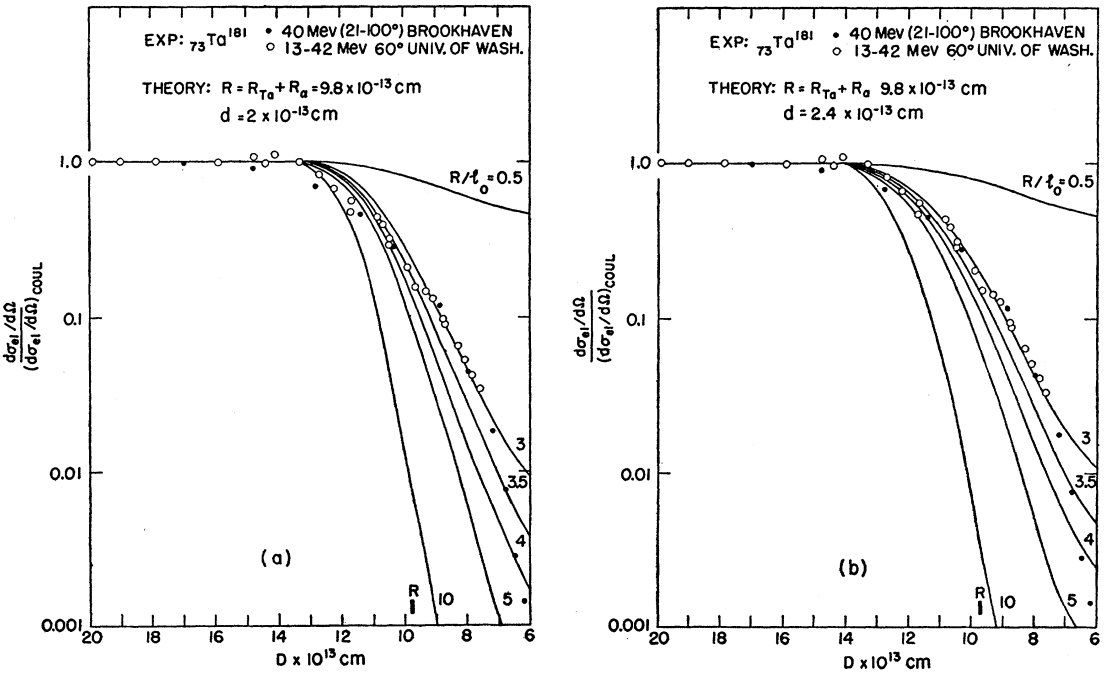


FIG. 4. Plot of differential elastic scattering cross section divided by the differential Coulomb cross section *versus* apsidal distance for $_{73}Ta^{181}$. The solid circles are data for 40-Mev alpha particles with scattering angles ranging from 21° to 100° (reference 4). The open circles are data for 13- to 42-Mev alpha particles at a scattering angle of 60° (reference 2). Theoretical curves are shown for $R=9.8\times10^{-13}$ cm, $R/l_0=0.5$, 3, 3.5, 4, 5, and 10, and (a) $d=2\times10^{-13}$ cm ($\delta=0.2$); (b) $d=2.4\times10^{-13}$ cm ($\delta=0.25$).

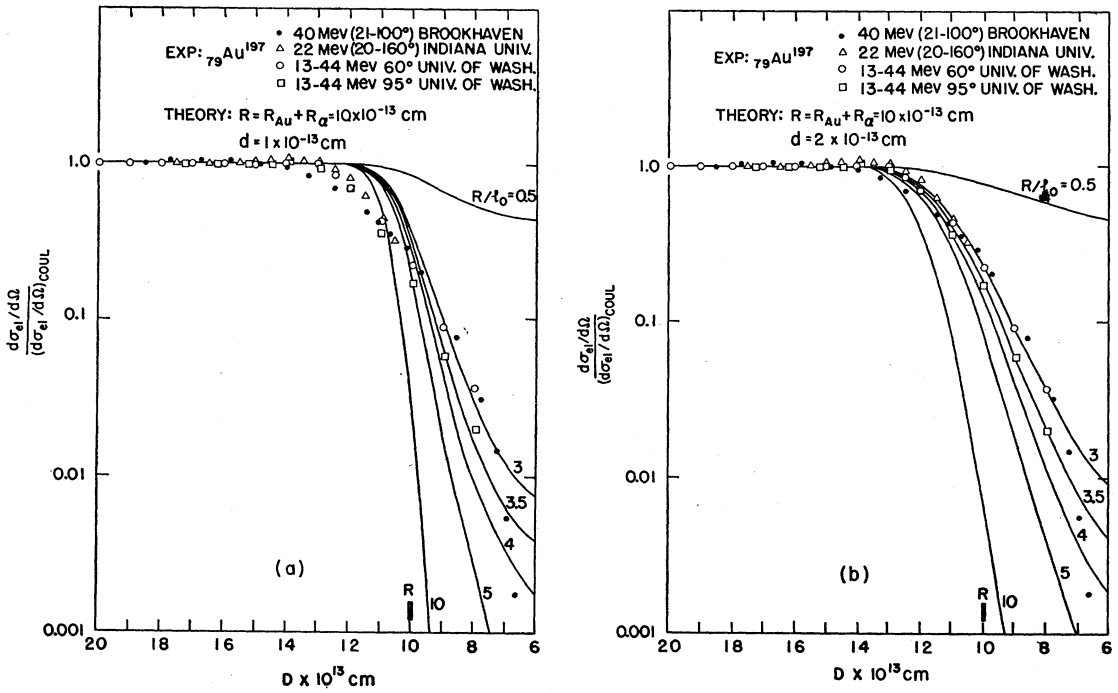


FIG. 5. Plot of differential elastic scattering cross section divided by the differential Coulomb cross section *versus* apsidal distance for $_{79}Au^{197}$. The solid circles are data for 40-Mev alpha particles with scattering angles ranging from 21° to 100° (reference 4). The triangles are data for 22-Mev alpha particles with scattering angles ranging from 20° to 160° (reference 3). The open circles are for 13- to 44-Mev alpha particles at a scattering angle of 60° (reference 2). The squares are for 13- to 44-Mev alpha particles at a scattering angle of 95° (reference 2). Theoretical curves are shown for $R=10\times10^{-13}$ cm, $R/l_0=0.5$, 3, 3.5, 4, 5, and 10, and (a) $d=1\times10^{-13}$ cm ($\delta=0.1$); (b) $d=2\times10^{-13}$ cm ($\delta=0.2$).

so that Eq. (4) becomes

$$\int \frac{dx}{l(x)}=\frac{2R}{l_0}\int_\xi^\infty dv(v^2-\xi^2)^{\frac{1}{2}}\,\mathrm{sech}^2\left(\frac{v-1}{\delta}\right), \quad (10)$$

$$\equiv(2R/l_0)h(\xi,\delta),$$

in which

$$\xi=D/R, \quad v=r/R, \quad \delta=d/R. \quad (11)$$

Figure 2 shows plots of $h(\xi,\delta)$ as a function of $\xi$ for $\delta=0$, 0.1, 0.2, and 0.25. [The integral in Eq. (10) can be calculated in closed form if $\mathrm{sech}^2[(v-1)/\delta]$ is approximated by a triangle, and this procedure is the one that was actually followed to obtain the curves in Fig. 2.]

## III. COMPARISON TO DATA

For a given choice of $\delta$ and $R$, one can plot from Eqs. (2) and (10) the transmission factor $T$ (the ratio of measured cross section to Coulomb cross section) as a function of apsidal distance $D$ for various values of $R/l_0$. This has been done for a number of elements for both alpha particle and deuteron elastic scattering in Figs. 3 to 8 which also contain the presently available data[5,9] for these elements. The figures have been arranged in ascending order of atomic weight and for each atomic weight in increasing order in $d$, the diffuseness parameter. Since logarithmic scales are used in these plots, the theoretical curves can be obtained by inverting Fig. 2 and applying the scale factor $(2R/l_0)$ to the ordinate $h$ and the scale factor $R$ to the abscissa $\xi$.

In all of the alpha-particle plots (Figs. 3 to 7) the interaction radius $R$ was obtained by assuming $R=R_A+R_\alpha$ with $R_A=1.51\times10^{-13}A^{\frac{1}{3}}$ cm and $R_\alpha=1.2\times10^{-13}$ cm. For the deuteron plots (Fig. 8), the interaction radius $R$ was varied with $\delta$ fixed, to try to improve the agreement between the calculated curves and the data.

Figure 3 shows alpha-particle apsidal-distance plots for Ag. The better agreement seems to be obtained for $d=2.1\times10^{-13}$ cm. In Ag the best value of $R/l_0$ is more uncertain than for the other elements shown in Figs. 4–7 since the energy and angular dependent data do not coincide if the transmission factor $T$ is less than 0.1. It does seem, however, that the best effective value of $R/l_0$ is between 2 and 4.

Figure 4 shows similar plots for Ta. In this case the better agreement seems to be obtained for $d=2.4\times10^{-13}$ cm with $R/l_0$ ranging from 3 to 4.

The best values of $d$ and $R/l_0$ for Au (Fig. 5) seem to be $d=2\times10^{-13}$ cm and $R/l_0\sim3$–4. These values also give good agreement for Pb (see Fig. 6). For Th (Fig. 7), $d=2.1\times10^{-13}$ cm and $R/l_0\sim3$–4 give a reasonable fit.

Figure 8 shows deuteron apsidal-distance plots for

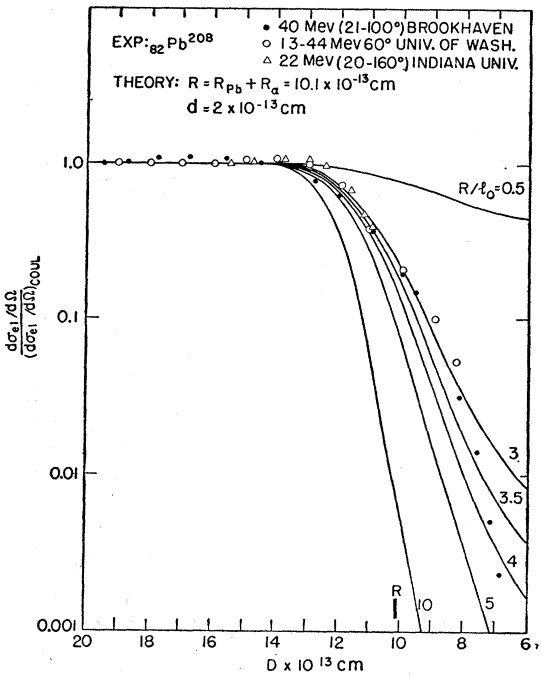


FIG. 6. Plot of the differential elastic scattering cross section divided by the differential Coulomb cross section *versus* apsidal distance for $_{82}Pb^{208}$. The solid circles are data for 40-Mev alpha particles with scattering angles ranging from 21° to 100° (reference 4). The open circles are data for 13- to 44-Mev alpha particles at a scattering angle of 60° (reference 2). The triangles are for 22-Mev alpha particles with scattering angles ranging from 20° to 160° (reference 3). The theoretical curves are shown for $R=10.1\times10^{-13}$ cm, $R/l_0=0.5$, 3, 3.5, 4, 5, and 10, and $d=2\times10^{-13}$ cm ($\delta=0.2$).

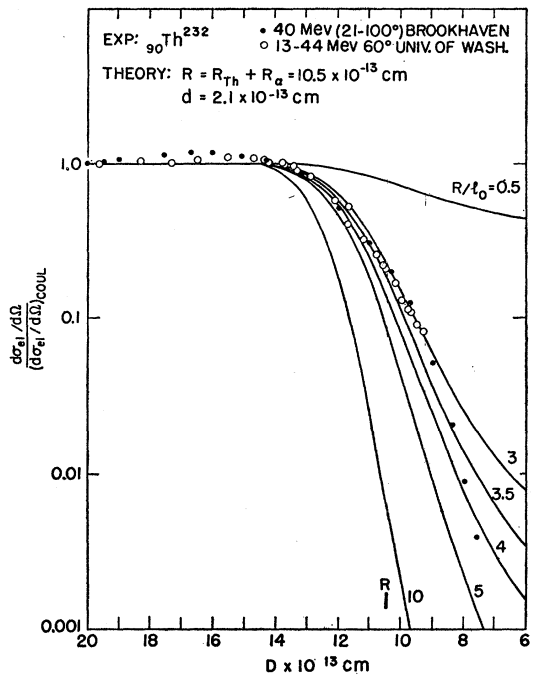


FIG. 7. Plot of the differential elastic scattering cross section divided by the differential Coulomb cross section *versus* apsidal distance for $_{90}Th^{232}$. The solid circles are data for 40-Mev alpha particles with scattering angles ranging from 21° to 100° (reference 4). The open circles are data for 13- to 44-Mev alpha particles at a scattering angle of 60° (reference 2). Theoretical curves are shown for $R=10.5\times10^{-13}$ cm, $R/l_0=0.5$, 3, 3.5, 4, 5, and 10, and $d=2.1\times10^{-13}$ cm ($\delta=0.2$).

Pb and Bi. The values $R=14\times10^{-13}$ cm and $d=3.5\times10^{-13}$ cm seem to agree best with the data although they appear to be rather large. If these values are taken seriously, the best value of $R/l_0$ seems to be about 1.

## IV. DISCUSSION

The best values of $d$ and $R/l_0$ assuming these parameters to be the same for all encounters of the alpha particle with other nuclear matter are $d\sim2\times10^{-13}$ cm and $R/l_0\sim$three to four, indicating that nuclei are completely opaque to alpha particles except in the region of density fall-off near the edge. Since the density of Eq. (6) falls off for large $r$ as $\exp[-2(r-R)/d]$, the $1/e$ distance is $(d/2)\sim1\times10^{-13}$ cm, a diffuseness about twice that found for protons.[11] This can be understood qualitatively if the diffuseness of the nucleon itself is assumed to be negligible. The diffuseness doubling in the alpha-particle experiments can then be said to arise because both the incident and target nuclei have about the same non-negligible diffuseness. For such short internal mean free paths as are indicated by the large values of $R/l_0$, the total reaction cross section is geometrical, i.e., $\sim\pi R^2$. Recent data[4] indicate that the cross section for neutron production in Au has about this value.

Interpretation of the deuteron data is somewhat uncertain in view of the possibility of electric breakup of the deuteron.[12–15] Such an effect might account for the "long-range" nature of the drop from Coulomb evident in Fig. 8. There is some indication of a more rapid fall-off at smaller apsidal distance which could be interpreted as the onset of nuclear effects although the available data do not extend to small enough apsidal distances to provide a firm basis for this view. Because the apsidal distance $D$ varies slowly with the scattering angle $\theta$ for $\theta>90°$, in order to get to smaller apsidal distances it is better to increase the incident energy if possible ($D$ varies inversely with energy) rather than to go to backward angles. It would be desirable to do this for both alpha particles and deuterons.

The use of straight line paths can be criticized, of course, since this procedure forces the dependence of $T$ on apsidal distance $D$ by equating $D$ to the impact parameter. However, $x(r)$ for straight line paths does exhibit two important features for any reasonable

[11] Melkanoff, Nodvik, Saxon, and Woods, private communication.

[12] The remarks in this paragraph are based on comments made by H. E. Wegner in a conversation with the writer.

[13] J. R. Oppenheimer, Phys. Rev. 47, 845 (1935).

[14] S. M. Dancoff, Phys. Rev. 72, 1017 (1947).

[15] C. J. Mullin and E. Guth, Phys. Rev. 82, 141 (1951).

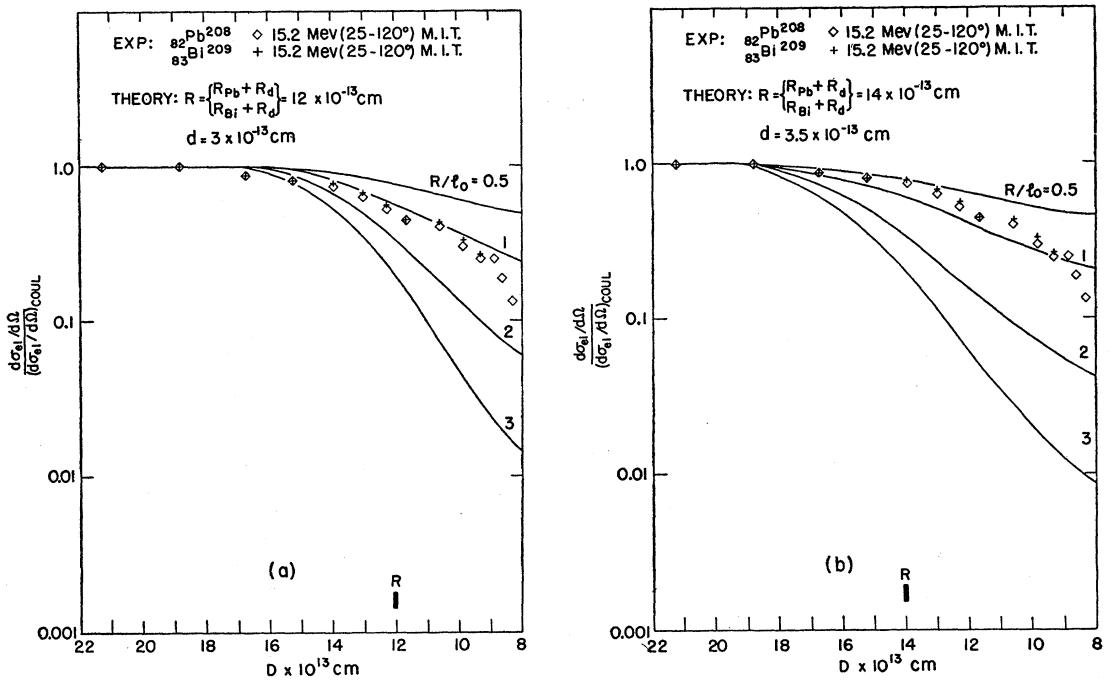


FIG. 8. Plot of differential elastic scattering cross section divided by the differential Coulomb cross section *versus* apsidal distance for $_{82}Pb^{208}$ and $_{83}Bi^{209}$. The diamonds are for 15.2-Mev deuterons on $_{82}Pb^{208}$ with scattering angles ranging from 25° to 120° (reference 5). The crosses are for 15.2-Mev deuterons on $_{83}Bi^{209}$ with scattering angles ranging from 25° to 120° (reference 5). Theoretical curves are shown for $R/l_0=0.5$, 1, 2, and 3, and (a) $R=12\times10^{-13}$ cm, $d=3\times10^{-13}$ cm ($\delta=0.25$); (b) $R=14\times10^{-13}$ cm, $d=3.5\times10^{-13}$ cm ($\delta=0.25$).

path, *viz.*,

$$x(r) \underset{r\to\infty}{\longrightarrow} r, \qquad (12)$$

$$\frac{dx}{dr} \underset{r\to D}{\longrightarrow} \infty.$$

Other paths should nevertheless be tried, especially since for Ag (see Fig. 3), the energy and angular dependent data do not coincide as well as for the other elements on an apsidal-distance plot. (The disagreement of the different types of data for Ag may be due to the fact that at smaller apsidal distances the angle at which the diffuse region is being crossed on a Coulomb trajectory is quite different for the two sets of data, even though the apsidal distances are the same.)

Distortion of the path by the nuclear forces is omitted in the form of Eq. (1). The alpha-particle data exhibit in some cases a rise before the rapid drop from Coulomb (see, e.g., Figs. 5–7). That this rise may come from refraction effects is indicated by the classical calculations of Hardmeier[16] for a real potential. It should be possible to ignore orbit distortion due to penetration of the charge distribution if the path of the incident particle runs through the neutron fringe suggested by Johnson and Teller[17] and supported by Hess.[18]

It is perhaps worth pointing out that recently reported results[19] on the decrease from Coulomb scattering encountered in the elastic scattering of nitrogen by nitrogen indicate a behavior analogous to the alpha particle and deuteron scattering.

If the physical picture discussed here is correct, namely that absorption is the most important feature in the drop from Coulomb scattering, it would seem that the model proposed by Ford and Wheeler[8] is based upon diffraction deviations from the wrong classical model. The fact that when their calculation is normalized to the Coulomb cross section the predicted drop from Coulomb is too rapid may indicate that their model is close to a classical model with a fairly sharp angular cutoff and that the diffraction effects they predict are not large enough to give much deviation from this angular cutoff.

## ACKNOWLEDGMENTS

The writer would like to thank H. E. Wegner for making available his apsidal distance plots and R. M. Eisberg, G. Igo, and H. E. Wegner for many discussions of both their data and the nature of the interaction of the alpha particle and deuteron with complex nuclei. He is indebted to V. F. Weisskopf for critical comment on the manuscript. In addition he wishes to thank Betty Oppenheim for carrying out the numerical calculations.

[16] W. Hardmeier, Physik. Z. **28**, 181 (1927), p. 187.
[17] M. H. Johnson and E. Teller, Phys. Rev. **93**, 357 (1954).
[18] W. N. Hess, thesis, University of California, UCRL-2670, 1954 (unpublished).
[19] H. L. Reynolds and A. Zucker, Bull. Am. Phys. Soc. **30**, No. 3, 40 (1955).